

# Optical model potential for deuteron elastic scattering with 1p-shell nuclei

Y. Zhang,<sup>1</sup> D. Y. Pang,<sup>2,3,\*</sup> and J. L. Lou<sup>1,†</sup>

<sup>1</sup>School of Physics and State Key Laboratory of Nuclear Physics and Technology, Peking University, Beijing 100871, China

<sup>2</sup>School of Physics and Nuclear Energy Engineering, Beihang University, Beijing 100191, China

<sup>3</sup>Beijing Key Laboratory of Advanced Nuclear Materials and Physics, Beihang University, Beijing 100191, China

(Received 5 June 2016; revised manuscript received 28 June 2016; published 29 July 2016)

A set of global optical potential parameters, DA1p, for deuterons with the 1p-shell nuclei is obtained by simultaneously fitting 67 sets of experimental data of deuteron elastic scattering from  $^6\text{Li}$ ,  $^9\text{Be}$ ,  $^{10}\text{B}$ ,  $^{11}\text{B}$ ,  $^{12}\text{C}$ ,  $^{13}\text{C}$ ,  $^{14}\text{N}$ ,  $^{16}\text{O}$ , and  $^{18}\text{O}$  with incident energies between 5.25 and 170 MeV. DA1p improves the description of the deuteron elastic scattering from the 1p-shell nuclei with respect to the existing systematic deuteron potentials and can give satisfactory reproduction of the experimental data with radiative nuclei such as  $^9\text{Li}$ ,  $^{10}\text{Be}$ ,  $^{14}\text{C}$ , and  $^{14}\text{O}$ .

DOI: 10.1103/PhysRevC.94.014619

## I. INTRODUCTION

Systematic optical model potentials (OMPs) are very useful in many fields of nuclear physics. They help to reduce the uncertainties of nuclear structure information extracted from direct nuclear reactions [1] and to make systematic analyses [2,3]. They are also indispensable in reliable predictions of reaction rates of direct nuclear reactions, which are not easy or impossible to be measured directly in laboratories. Over the past several decades, many systematic potentials have been proposed for nucleons ( $A = 1$ ) [4–7], deuterons ( $A = 2$ ) [8–12],  $^3\text{H}$  and  $^3\text{He}$  ( $A = 3$ ) [13–17],  $\alpha$  particles ( $A = 4$ ) [18–21], and heavy ions ( $A \geq 6$ ) [22–24]. They are widely used in studies of direct nuclear reactions.

While the study of deuteron interactions with a range of targets can help us understand their dependence on the internal structure of the targets, they are also needed for reaction studies such as  $(d, p)$ ,  $(d, n)$ , and  $(^3\text{He}, d)$  where the optical potentials are needed for analyses that rely on the distorted-wave Born approximation for extracting nuclear structure information [25,26]. Deuteron optical potentials are also needed in reactions induced by radiative nuclei with a deuterium target in inverse kinematics. In such reactions, one usually focuses on the weakly bound nature of the radiative nuclei and needs the deuteron potential with the core nucleus in calculations with the continuum-discretized coupled-channel (CDCC) method [27].

Most of the existing systematic deuteron potentials are based on the analysis of angular distributions of elastic scattering cross sections of deuterons from heavy targets with atomic masses of, typically,  $A_T \gtrsim 30$  [8–10]. It is well known that the systematics developed at such heavy-mass regions are different from that in the light-mass regions ( $A_T \lesssim 20$ ) [28,29]. Phenomenological renormalization factors are found to be necessary when systematic potentials developed in the heavy-mass region are applied to light targets [27,30]. This is not convenient in theoretical calculations for reactions that

have no corresponding elastic scattering data to constrain the OMP parameters. The database for the systematics of Han *et al.* [11] and An and Cai [12] include  $^{12}\text{C}$ ,  $^{14}\text{N}$ , and  $^{16}\text{O}$  targets. However, their systematics are not optimized for the light-target region. Many experimental data with other light-heavy targets are not included. It is thus very useful to establish a systematic deuteron potential for the 1p-shell nuclei.

In this article, we report a systematic deuteron potential with the 1p-shell nuclei. It is designated as DA1p. The target nuclei include  $^6\text{Li}$ ,  $^9\text{Be}$ ,  $^{10}\text{B}$ ,  $^{11}\text{B}$ ,  $^{12}\text{C}$ ,  $^{13}\text{C}$ ,  $^{14}\text{N}$ ,  $^{16}\text{O}$ , and  $^{18}\text{O}$  with deuteron incident energies between 5.25 and 170 MeV. The experimental data available for the  $^6\text{Li}$  and  $^7\text{Li}$  targets are mostly limited for deuteron energies below 14.7 MeV. Within this energy region, contributions to the scattering from their underlying cluster structure make deuteron scattering from these two nuclei require a separate analysis when compared with the heavier 1p-shell nuclei. The parametrization of DA1p is described in Sec. II A; the resulting OMP parameters are reported in Sec. II B with comparisons between optical model calculations and experimental data. Examination of the application of DA1p to the total cross sections and elastic scattering from radiative nuclei is presented in Sec. III. Our conclusions are given in Sec. IV.

## II. PARAMETERIZATION AND DETERMINATION OF THE SYSTEMATIC POTENTIAL PARAMETERS

### A. Parameterization

The parametrization of the optical model potential,  $U(r)$ , as a function of  $r$ , which is the distance between a projectile nucleus and a target nucleus, is the same as that of HT1p [29]:

$$U(r) = -V_v f_{ws}(r, R_r, a_r) - i W_v f_{ws}(r, R_w, a_w) - i W_s (-4a_w) \frac{d}{dr} f_{ws}(r, R_w, a_w) + V_C(r), \quad (1)$$

where  $V_v$ ,  $W_v$ , and  $W_s$  are the depths of the real potentials and the volume and surface imaginary potentials, respectively.  $f_{ws}(r)$  is the Woods-Saxon form factor:

$$f_{ws}(r, R_i, a_i) = \frac{1}{1 + \exp [(r - R_i)/a_i]}, \quad (2)$$

\*Corresponding author: dypang@buaa.edu.cn

†Corresponding author: jlou@pku.edu.cn

TABLE I. The database used in searching for the parameters of DA1p. The  $\chi^2$  values with the systematics of DA1p, Daehnick *et al.* [10], and An and Cai [12] are labeled as  $\chi^2_{\text{DA1p}}$ ,  $\chi^2_{\text{Dae}}$ , and  $\chi^2_{\text{An}}$ , respectively. The  $\chi^2_{\text{DA1p}}$  values are calculated with their corresponding  $N_o$  values, which are normalization factors of the experimental data, while the  $\chi^2_{\text{Dae}}$  and  $\chi^2_{\text{An}}$  values are not. The unit of  $E_d$  is MeV.

Target	$E_d$	$\chi^2_{\text{DA1p}}$	$N_o$	$\chi^2_{\text{Dae}}$	$\chi^2_{\text{An}}$	Ref.	Target	$E_d$	$\chi^2_{\text{DA1p}}$	$N_o$	$\chi^2_{\text{Dae}}$	$\chi^2_{\text{An}}$	Ref.	Target	$E_d$	$\chi^2_{\text{DA1p}}$	$N_o$	$\chi^2_{\text{Dae}}$	$\chi^2_{\text{An}}$	Ref.
<sup>6</sup> Li	4.5	0.46	1.09	18	17	[33]	<sup>9</sup> Be	7	1.7	1.17	20	17	[34]	<sup>12</sup> C	25.9	6.5	1.23	8.8	8.8	[35]
	4.75	1.5	1.04	18	17	[33]		7.5	2.2	1.00	12	10	[36]		29.5	9.9	1.08	5.6	4.7	[37]
	5	1.7	1.02	23	22	[33]		8	2.4	0.927	13	11	[36]		34.4	1.3	0.855	1.4	2.6	[38]
	5.25	1.8	0.993	26	25	[33]		8.5	4.0	0.906	19	16	[36]		52	0.88	0.772	1.3	2.5	[39]
	6	6.2	1.06	26	26	[40]		9	2.5	0.776	11	9.7	[36]		53.3	0.80	0.672	2.6	2.6	[41]
	7	5.1	1.14	26	26	[40]		9.5	3.0	0.787	14	12	[36]		56	2.5	0.765	3.5	7.3	[42]
	8	3.5	1.07	28	28	[40]		11.8	7.5	1.01	42	38	[43]		60.6	3.0	0.998	10	3.4	[44]
	8	3.0	0.994	25	25	[45]		13.6	8.5	0.924	24	22	[46]		77.3	0.72	1.06	8.5	2.1	[44]
	9	1.2	0.991	27	27	[40]		15	11	1.22	42	40	[47]		80	0.68	0.953	3.6	1.7	[48]
	10	0.5	0.870	26	25	[40]		15.8	8.0	1.03	30	29	[49]		90	0.60	1.33	29	7.7	[44]
	10	0.9	0.920	28	28	[45]		24	5.0	1.21	22	25	[50]		110	0.58	1.09	12	1.3	[51]
	11.8	1.6	0.938	28	27	[52]		27.7	4.2	1.08	3.8	7.0	[53]		120	1.1	0.961	6.4	2.4	[51]
	12	2.1	0.946	30	29	[45]	<sup>10</sup> B	11.8	4.6	0.961	12	11	[43]	<sup>14</sup> N	11.8	2.2	0.880	10	7.5	[43]
<sup>7</sup> Li	14.7	5.4	1.33	19	19	[55]	<sup>11</sup> B	11.8	3.5	1.27	42	32	[43]	<sup>17</sup> O	4.8	1.15	10	5.6	[56]	
	25	3.7	1.01	5.6	14	[57]		13.6	2.9	1.30	22	19	[46]	<sup>13</sup> C	13.7	7.9	0.904	16	14	[58]
	171	1.4	1.01	14	14	[59]		27.7	4.4	1.02	2.9	3.0	[53]		17.7	2.9	0.700	19	12	[60]
	6	3.0	0.884	30	30	[40]	<sup>12</sup> C	7	2.4	0.707	14	14	[61]	<sup>14</sup> N	11.8	2.2	0.880	10	7.5	[43]
	7	1.9	0.982	30	30	[40]		8	1.4	1.28	17	14	[61]		52	2.7	0.767	2.9	5.3	[39]
	8	0.93	0.999	30	30	[40]		9	2.8	0.887	13	11	[61]	<sup>16</sup> O	5.25	1.3	0.839	5.7	6.6	[62]
	9	0.64	0.936	31	30	[40]		10.6	3.2	1.05	13	9.6	[63]		5.5	0.63	0.869	4.6	5.4	[62]
	10	0.81	0.902	32	32	[40]		11	5.4	0.929	14	12	[63]		6	2.8	1.17	5.5	6.4	[62]
	11.8	1.2	1.08	34	33	[52]		11	3.8	0.970	19	15	[61]		11.8	1.5	1.06	13	8.3	[43]
	12	1.2	0.926	27	26	[45]		11.4	3.8	1.01	15	11	[63]		13.3	6.6	0.973	7.2	6.1	[64]
	14.7	1.2	0.962	24	24	[55]		11.8	4.5	1.19	34	23	[43]		15.8	6.8	1.13	9.6	8.4	[49]
	5.5	1.7	0.707	12	11	[33]		12.4	3.3	1.04	11	9.5	[63]		34.4	4.0	0.947	4.6	5.9	[38]
	5.75	0.95	0.718	12	10	[33]		12.8	6.8	0.785	14	14	[63]		52	1.9	1.30	8.5	1.7	[39]
	6	3.0	1.11	7.1	7.4	[36]		13.2	6.6	0.689	20	19	[63]		56	3.6	1.01	1.6	4.5	[65]
	6	4.3	1.01	4.7	4.4	[33]		13.9	6.6	0.848	15	15	[63]		171	4.8	0.976	3.1	3.6	[59]
	6.5	2.7	1.06	8.0	7.8	[36]		15.3	11	1.18	59	50	[66]	<sup>18</sup> O	16.3	1.6	1.10	7.3	5.9	[67]
	7	1.7	1.08	12	11	[36]		15.8	7.6	0.966	37	30	[49]							

with  $i = r$  and  $w$  for the real and imaginary potentials, respectively.

The diffuseness of these potentials is assumed to be independent of the target masses ( $A_T$ ) and incident energies ( $E$  in MeV). Such dependencies, however, are parametrized in the radius parameters:

$$R_i = r_i A_T^{1/3} + r_i^{(0)} + r_{ie}(E - E_C), \quad (3)$$

where  $E_C$  is the Coulomb correction to the incident energy [5,8,15]:

$$E_C = \frac{6Z_P Z_T e^2}{5R_C}, \quad (4)$$

in which,  $e^2 = 1.44$  MeV fm,  $Z_T$  and  $Z_P$  are the charge numbers of the target and the projectile nuclei, respectively, and  $R_C = r_c A_T^{1/3}$  is the radius of the Coulomb potential:

$$V_C(r) = \begin{cases} \frac{Z_P Z_T e^2}{r} & (r \geq R_C), \\ \frac{Z_P Z_T e^2}{2R_C} \left(3 - \frac{r^2}{R_C^2}\right) & (r \leq R_C). \end{cases} \quad (5)$$

In this work  $r_c$  is fixed to be 1.3 fm. The energy dependence of the radius parameters for both the real and the imaginary

parts are found to be important to simultaneously describe the elastic scattering data in a wide energy range, as suggested in Ref. [20].

The depth of the real potential in Eq. (1) is assumed to depend linearly on the incident energies:

$$V_v(E) = V_r + V_e(E - E_C). \quad (6)$$

The volume and surface terms of the imaginary potentials,  $W_v$  and  $W_s$ , are defined as

$$W_v(E) = \frac{W_{v0}}{1 + \exp\left(\frac{W_{ve0} - (E - E_C)}{W_{vew}}\right)}, \quad (7)$$

$$W_s(E) = \frac{W_{s0}}{1 + \exp\left(\frac{(E - E_C) - W_{se0}}{W_{srew}}\right)}. \quad (8)$$

For <sup>6,7</sup>Li at low energies, the imaginary potentials are assumed to depend linearly on the incident energies:  $W_j = W_{j0} + W_{je}(E - E_C)$ , with  $j = v$  and  $s$  for the volume and surface imaginary parts, respectively.

Spin-orbit potentials are not included in the parametrization of DA1p. We do this because of two practical reasons. First, we expect DA1p to be used in CDCC calculations

for reactions induced by weakly bound radiative nuclei with the deuterium targets. Currently, in most CDCC calculations using, for example, the computer code FRESCO [31], spin-orbit couplings are not implemented. In such cases we need the OMP of the deuteron to reproduce the elastic scattering data without a spin-orbit potential as well. Second, the experimental data analyzed in this work are all angular distributions of elastic scattering cross sections, which are not sensitive to the spin-orbit potentials, especially at forward angles, where the data are most well accounted for by the optical model. In total we have 16 free parameters for DA1p, which are listed in Table II.

### B. Parameters of DA1p and comparisons with experimental data

Eighty-nine sets of experimental data for deuteron elastic scattering from the  $1p$ -shell nuclei are analyzed in this work, which consist of 65 sets for  $^9\text{Be}$ ,  $^{10,11}\text{B}$ ,  $^{12,13}\text{C}$ ,  $^{14}\text{N}$ , and  $^{16,18}\text{O}$  with incident energies below 171 MeV and 24 sets for  $^{6,7}\text{Li}$  from 4.5 to 171 MeV. All the data sets are obtained from the EXFOR database [32]. Details of these data are shown in Table I.

In searching for the parameters of DA1p, 65 sets of data for the  $^9\text{Be}$ ,  $^{10,11}\text{B}$ ,  $^{12,13}\text{C}$ ,  $^{14}\text{N}$ , and  $^{16,18}\text{O}$  targets together with the two sets of  $^6\text{Li}$  at 25 and 171 MeV are simultaneously fitted using the computer code MINOPT [5]. The OMP parameters are optimized with the usual minimization of the  $\chi^2$  method:

$$\chi^2 = \frac{1}{N} \sum_{i=1}^N \frac{[\sigma_i^{\text{exp}} - \sigma_i^{\text{th}}]^2}{\Delta\sigma_i^2}, \quad (9)$$

where  $\sigma_i^{\text{exp}}$ ,  $\sigma_i^{\text{th}}$ , and  $\Delta\sigma_i$  are the experimental and theoretical cross sections and the experimental errors, respectively. Uniform uncertainty of the experimental data  $\Delta\sigma_i/\sigma_i^{\text{exp}} = 15\%$  is assumed in this work. Experimental data measured by different groups may have different systematic uncertainties. For this reason, normalization of the experimental data is allowed during the parameter searching with MINOPT [5]. The corresponding normalization factors  $N_o$  are listed in Table I. In most of the cases the values of  $N_o$  are close to unity. Convergence of the searching is ensured by observing that the values of parameters came back to their optimized ones (within their uncertainties) in fittings with different initial values randomly set within 10%. The uncertainties of the parameters of DA1p are obtained with the bootstrap method [68], which reduplicates the calculations 1000 times by random sampling with replacements of the data sets used in the original database. Details of applying the bootstrap method for the uncertainties of the systematic OMPs can be found in Refs. [5,15]. The final parameters of DA1p and their uncertainties are given in Table II.

During this work, we found that the experimental data of  $^6\text{Li}$  and  $^7\text{Li}$  at low incident energies ( $E < 15$  MeV) are hard to be described together with the other data sets using one systematic potential. These data may have considerable contributions from other reaction channels due to their cluster structure, which cannot be accounted for by the optical model

TABLE II. Values of parameters,  $P$ , and their uncertainties,  $\Delta P$ , of DA1p.  $V_r$ ,  $V_e$ ,  $W_{v0}$ ,  $W_{s0}$ ,  $W_{se}$ ,  $W_{ve0}$ ,  $W_{vew}$ ,  $W_{se0}$ , and  $W_{sew}$  are in MeV, and  $r_r$ ,  $r_r^{(0)}$ ,  $r_{re}$ ,  $a_r$ ,  $r_w$ ,  $r_w^{(0)}$ ,  $r_{we}$ , and  $a_w$  are in femtometers.

Parameter	$1p$ shell		$^6\text{Li}$		$^7\text{Li}$	
	$P$	$\Delta P$	$P$	$\Delta P$	$P$	$\Delta P$
$V_r$	98.9	0.8	47.9	1.5	26.1	0.7
$V_e$	-0.279	0.021	2.37	0.17	1.19	0.02
$r_r$	1.11	0.001	1.62	0.01	1.45	0.01
$r_r^{(0)}$	-0.167	0.004				
$r_{re}$	0.001 17	0.000 09	-0.0122	0.0021	0.097	0.005
$a_r$	0.776	0.001	0.876	0.037	0.844	0.008
$W_{v0}$	11.5	0.7				
$W_{s0}$	7.56	0.67	11.3	0.8	215.0	0.2
$r_w$	0.561	0.006	2.83	0.039	2.12	0.02
$r_w^{(0)}$	3.07	0.002				
$r_{we}$	-0.004 49	0.000 08	-0.0911	0.0002	0.022	0.003
$a_w$	0.744	0.001	0.27	0.004	0.261	0.104
$W_{se}$			3.44	0.32	-16.1	0.1
$W_{ve0}$	18.1	1.4				
$W_{vew}$	5.97	1.33				
$W_{se0}$	14.3	1.4				
$W_{sew}$	4.55	0.86				

implemented in MINOPT. We search for the deuteron potentials with  $^6\text{Li}$  and  $^7\text{Li}$  at low energies separately. The results are also given in Table II. As one can see, the parameters of these two targets differ very much from the systematics established by the other  $1p$ -shell nuclei.

Comparisons between experimental data and optical model calculations of the DA1p parameters are given in Figs. 1–4

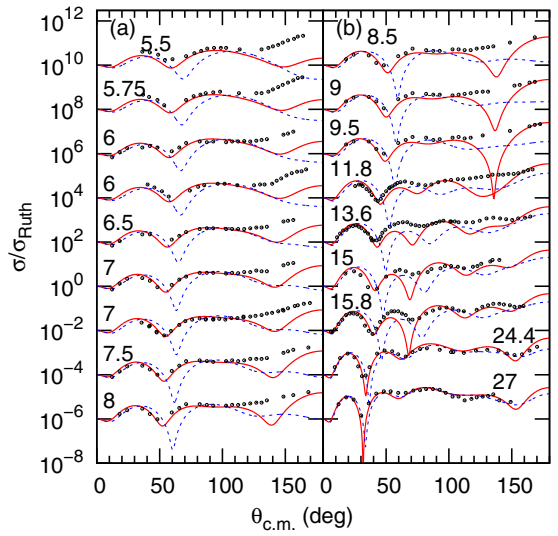


FIG. 1. Comparisons between the experimental data and optical model calculations with DA1p (solid curves) and Daehnick *et al.* [10] (dashed curves) for deuterons impinging on  $^9\text{Be}$ . The deuteron incident energies are indicated along with the curves in MeV. The cross sections are offset by factors of  $10^2$ .

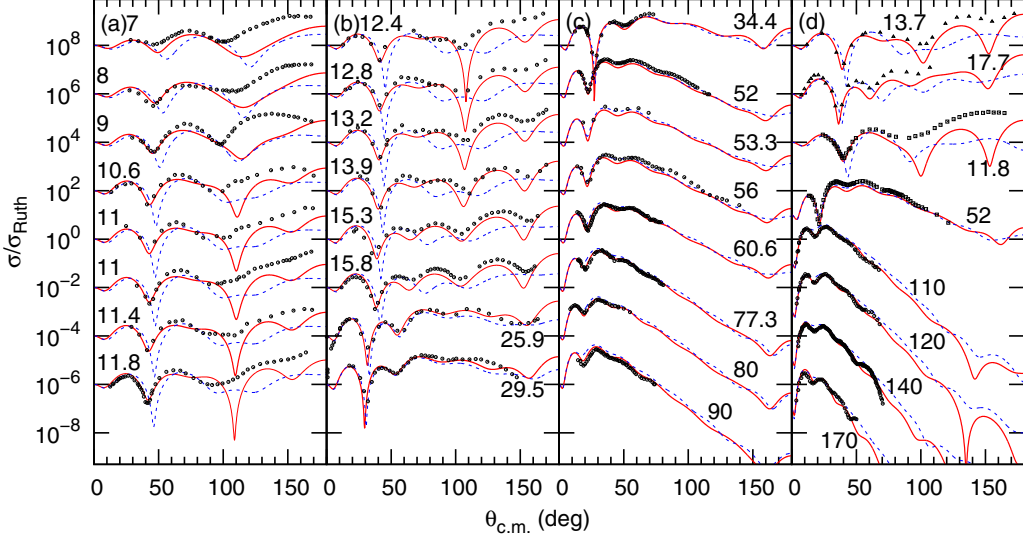


FIG. 2. The same as Fig. 1 but for deuteron elastic scattering from (a,b,c)  $^{12}\text{C}$  (circles) and (d)  $^{13}\text{C}$  (triangles),  $^{14}\text{N}$  (squares), and  $^{12}\text{C}$  (circles).

together with the predictions using the systematics of Daehnick *et al.* [10]. Clearly, DA1p improves the reproduction of the experimental data with respect to that of the latter, especially at low incident energies and at forward angles. At higher incident energies above around 30 MeV, both systematic potentials give satisfactory reproduction of the experimental data. A close comparison between the optical model calculations using these two systematic potentials at higher incident energies is given in Fig. 5. One sees that DA1p is better than the systematics of Daehnick *et al.* [10] in reproducing more details of the angular distributions of the experimental data. In addition, the  $\chi^2$  values associated with calculations using parameters of DA1p, of Daehnick *et al.* [10], and of An and Cai [12] are

also given in Table I. All  $\chi^2$  values are calculated assuming the same experimental uncertainties. Note that DA1p does not include spin-orbit potentials while the other two systematics do. In this sense, DA1p implicitly includes the effects of the spin-orbit potential.

It is interesting to observe that the depth of the real part of DA1p, which has  $V_r = 98.9$  MeV, is larger than those in the systematics established for heavy targets, for example, the values of  $V_r$  are 86, 91.85, and 82.18 MeV in the work of Daehnick *et al.* [10], An and Cai [12], and Han *et al.* [11], respectively. The same differences between systematic potentials in 1  $p$ -shell nuclei and heavy-target nuclei are also found for protons and  $^3\text{H}$  and  $^3\text{He}$  [28,29]. Also, the radius parameter of the imaginary potential,  $r_w^{(0)}$ , as shown in

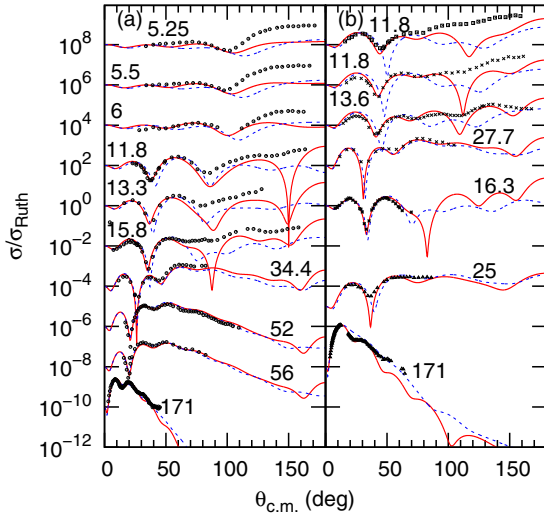


FIG. 3. The same as Fig. 1 but for deuteron elastic scattering from (a)  $^{16}\text{O}$  (circles) and (b)  $^{10}\text{B}$  (squares),  $^{11}\text{B}$  (x's),  $^{18}\text{O}$  (asterisks), and  $^6\text{Li}$  (triangles) at high energy.

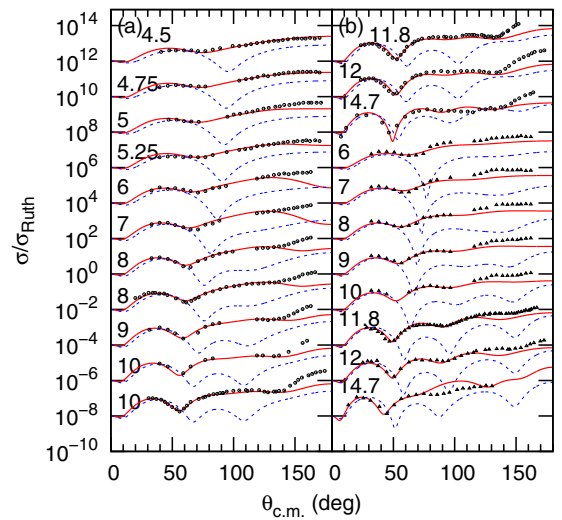


FIG. 4. The same as Fig. 1 but for deuteron elastic scattering from  $^6\text{Li}$  (circles) and  $^7\text{Li}$  (triangles) at  $E_d < 15$  MeV.

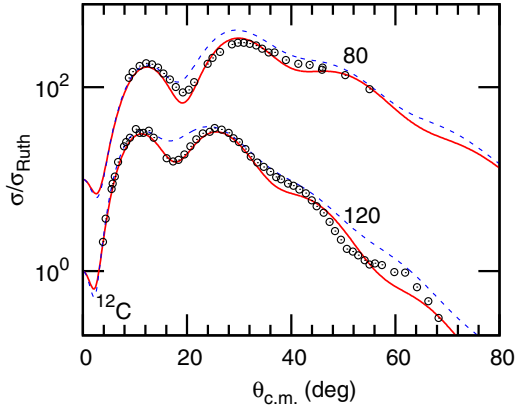


FIG. 5. Comparisons with optical model calculations and experimental data for deuteron elastic scattering from  $^{12}\text{C}$  at 80 and 120 MeV, separately plotted from Fig. 2 to show in detail comparisons between results with DA1p (solid curves) and those of Daehnick *et al.* [10] (dashed curves).

Table II, shows stronger dependence on the target masses than the systematics established in the heavy-target region. This may be related to the fact that the 1  $p$ -shell nuclei distinguish among each other more strongly than those among the heavy targets in their structures.

### III. APPLICATION OF DA1P TO RADIATIVE NUCLEI AND TOTAL REACTION CROSS SECTIONS

Comparisons between optical model calculations using DA1p and the experimental data that are not included in our database, mostly with radiative nuclei, are given in Fig. 6. Again, one sees that DA1p improves the reproduction of the

TABLE III. The same as Table I, but for the experimental data shown in Fig. 6.

Target	$E_d$	$\chi^2_{\text{DA1p}}$	$\chi^2_{\text{Dae}}$	$\chi^2_{\text{An}}$	Ref.
$^9\text{Li}$	10	5.11	4.37	4.21	[69]
$^{10}\text{Be}$	12	20.6	262	163	[70]
	15	9.22	94.9	65.0	[70]
	18	3.55	31.7	25.7	[70]
	21.4	10.4	147	126	[70]
	53.8	3.80	10.5	7.19	[71]
$^{11}\text{Be}$	17.06	4.10	6.17	4.31	[72]
$^{14}\text{C}$	35.6	4.06	4.67	6.06	[73]
$^{15}\text{N}$	15	14.4	12.9	13.0	[74]

experimental data with respect to the systematic potential of Daehnick *et al.* [10]. A detailed comparison of  $\chi^2$  values is given in Table III. This suggests that DA1p can give more reliable predictions to the elastic scattering cross sections of deuteron with nuclei that are away from the  $\beta$ -stability line.

Total reaction cross sections are not used to constrain the parameters of DA1p. Comparisons between optical model calculations and experimental data of total reaction cross sections are made for  $^9\text{Be}$ ,  $^{12}\text{C}$ , and  $^{16}\text{O}$  targets for deuteron incident energies of 37.9, 65.5, and 97.4 MeV [75] (see Fig. 7). Systematic potentials of DA1p, An and Cai [12], and Daehnick *et al.* [10] are used here. These results seem to suggest that the systematics of An and Cai [12] and Daehnick *et al.* [10] give better accounts of the total reaction cross sections of deuterons with light targets. However, we found that the discrepancies between results with DA1p and the experimental data might be reconciled when the breakup of deuterons is taken into account. We will discuss this problem in detail in a future article.

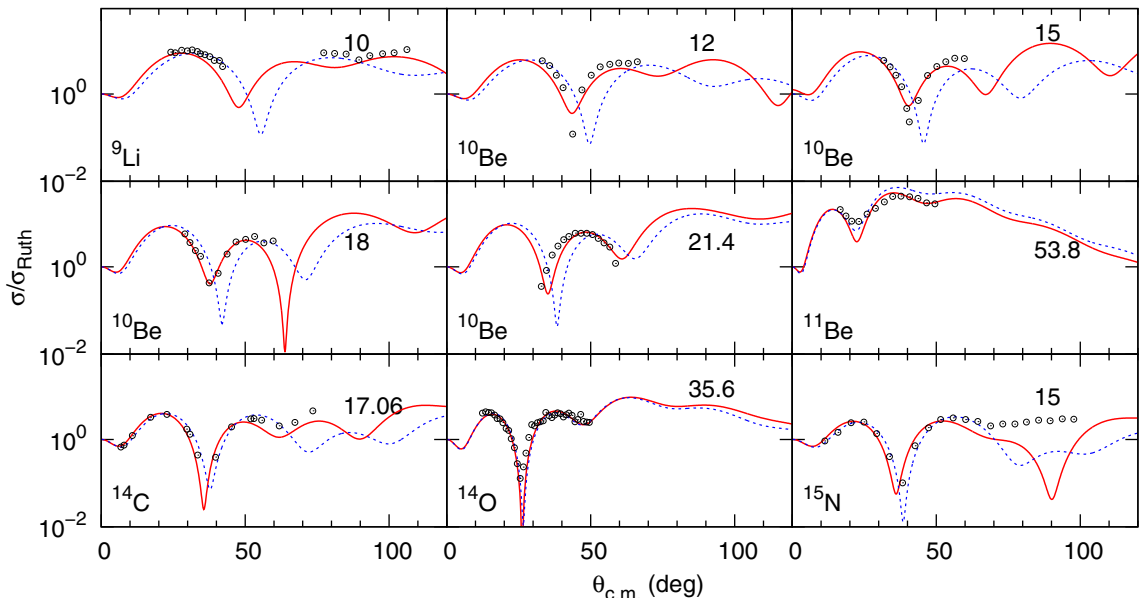


FIG. 6. The same as Fig. 1 but for experimental data that are not included in our systematic analysis, mostly for radiative nuclei [69–74].

## IV. CONCLUSIONS

In conclusion, we present in this article a systematic phenomenological optical model potential, DA1p, of deuterons with the  $1p$ -shell nuclei (except for  $^6\text{Li}$  and  $^7\text{Li}$ ) for incident energies from around 5 to 170 MeV. Two sets of parameters are given for  $^6\text{Li}$  and  $^7\text{Li}$  targets for incident energies between around 5 and 15 MeV. Differences in the potential parameters are found between DA1p and the systematic potentials established for heavy-target regions. DA1p is found to give satisfactory reproduction of the angular distributions of deuteron elastic scattering from both stable and radiative  $1p$ -shell nuclei. The experimental total reaction cross sections for  $^9\text{Be}$ ,  $^{12}\text{C}$ , and  $^{16}\text{O}$  targets are found to be overpredicted by theoretical calculations with systematic deuteron potentials, which may be due to the breakup of deuterons and will be further studied in a future article.

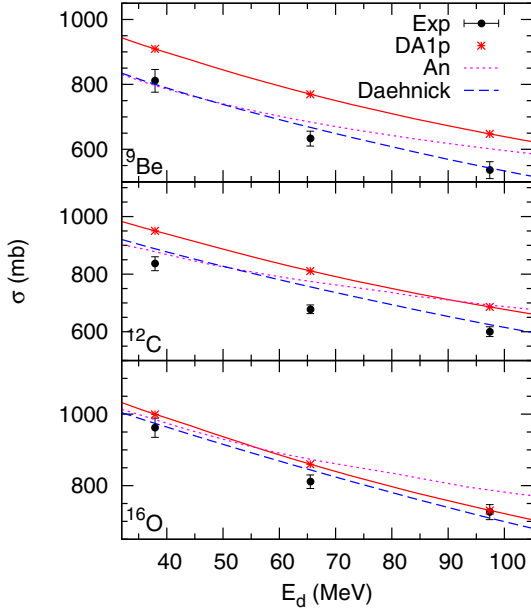


FIG. 7. Optical model calculations of the total reaction cross sections with systematics of DA1p, Daehnick *et al.* [10], and An and Cai [12] for targets  $^9\text{Be}$  (upper panel),  $^{12}\text{C}$  (middle panel), and  $^{16}\text{O}$  (bottom panel) and their comparisons with the experimental data [75].

## ACKNOWLEDGMENTS

The authors thank the anonymous referee for useful comments and suggestions. This work is supported by the 973 Program of China (Grant No. 2013CB834402), the National Natural Science Foundation of China (Grants No. 11275001, No. 11275018, No. U1432247, and No. 11535004) and the national key research and development program (2016YFA0400502).

- 
- [1] X. D. Liu, M. A. Famiano, W. G. Lynch, M. B. Tsang, and J. A. Tostevin, *Phys. Rev. C* **69**, 064313 (2004).  
[2] M. B. Tsang, J. Lee, and W. G. Lynch, *Phys. Rev. Lett.* **95**, 222501 (2005).  
[3] M. B. Tsang, J. Lee, S. C. Su *et al.*, *Phys. Rev. Lett.* **102**, 062501 (2009).  
[4] F. D. Becchetti, Jr., and G. W. Greenless, *Phys. Rev.* **182**, 1190 (1969).  
[5] R. L. Varner, W. J. Thompson, T. L. McAbee, E. J. Ludwig, and T. B. Clegg, *Phys. Rep.* **201**, 57 (1991).  
[6] A. J. Koning and J. P. Delaroche, *Nucl. Phys. A* **713**, 231 (2003).  
[7] R. Xu, Z. Ma, E. N. E. van Dalen, and H. Müther, *Phys. Rev. C* **85**, 034613 (2012).  
[8] C. M. Perey and F. G. Perey, *Phys. Rev.* **132**, 755 (1963).  
[9] J. M. Lohr and W. Haeberli, *Nucl. Phys. A* **232**, 381 (1984).  
[10] W. W. Daehnick, J. D. Childs, and Z. Vrcelj, *Phys. Rev. C* **21**, 2253 (1980).  
[11] Y. Han, Y. Shi, and Q. Shen, *Phys. Rev. C* **74**, 044615 (2006).  
[12] H. X. An and C. H. Cai, *Phys. Rev. C* **73**, 054605 (2006).  
[13] F. D. Becchetti, Jr., and G. W. Greenlees, in *Polarization Phenomena in Nuclear Reactions*, edited by H. H. Barschall and W. Haeberli (University of Wisconsin, Madison, WI, 1971), p. 682.  
[14] H. Guo, Y. Zhang, Y. Han, and Q. Shen, *Phys. Rev. C* **79**, 064601 (2009).  
[15] D. Y. Pang, P. Roussel-Chomaz, H. Savajols, R. L. Varner, and R. Wolski, *Phys. Rev. C* **79**, 024615 (2009).  
[16] X. Li, C. Liang, and C. Cai, *Nucl. Phys. A* **789**, 103 (2007).  
[17] C.-T. Liang, X.-H. Li, and C.-H. Cai, *J. Phys. G: Nucl. Part. Phys.* **36**, 085104 (2009).  
[18] M. Nolte, H. Machner, and J. Bojowald, *Phys. Rev. C* **36**, 1312 (1987).  
[19] M. Avrigeanu, A. C. Obreja, F. L. Roman, V. Avrigeanu, and W. von Oertzen, *At. Data Nucl. Data Tables* **95**, 501 (2009).  
[20] D. Y. Pang, Y. L. Ye, and F. R. Xu, *Phys. Rev. C* **83**, 064619 (2011).  
[21] D. Y. Pang, Y. L. Ye, and F. R. Xu, *J. Phys. G: Nucl. Part. Phys.* **39**, 095101 (2012).  
[22] L. C. Chamon, B. V. Carlson, L. R. Gasques *et al.*, *Phys. Rev. C* **66**, 014610 (2002).  
[23] T. Furumoto, W. Horiuchi, M. Takashina, Y. Yamamoto, and Y. Sakuragi, *Phys. Rev. C* **85**, 044607 (2012).  
[24] Y. P. Xu and D. Y. Pang, *Phys. Rev. C* **87**, 044605 (2013).  
[25] J. Vernotte, G. Berrier-Ronsin, J. Kalifa, R. Tamisier, and B. H. Wildenthal, *Nucl. Phys. A* **571**, 1 (1994).  
[26] J. Lee, P. Dan-Yang, H. Yin-Lu, and M. B. Tsang, *Chin. Phys. Lett.* **31**, 092103 (2014).  
[27] J. Chen, J. L. Lou, Y. L. Ye *et al.*, *Phys. Rev. C* **93**, 034623 (2016).  
[28] B. A. Watson, P. P. Singh, and R. E. Segel, *Phys. Rev.* **182**, 977 (1969).  
[29] D. Y. Pang, W. M. Dean, and A. M. Mukhamedzhanov, *Phys. Rev. C* **91**, 024611 (2015).  
[30] F. Jamil-Qureshi, L. Jian-Ling, Y. Yan-Lin *et al.*, *Chin. Phys. Lett.* **27**, 092501 (2010).  
[31] I. J. Thompson, *Comput. Phys. Rep.* **7**, 167 (1988).  
[32] N. Otuka, E. Dupont, V. Semkova *et al.*, *Nucl. Data Sheets* **120**, 272 (2014).  
[33] D. L. Powell, G. M. Crawley, B. V. N. Rao *et al.*, *Nucl. Phys. A* **147**, 65 (1970).

- [34] A. Szczurek, K. Bodek, J. Krug *et al.*, *Z. Phys. A* **333**, 271 (1989).
- [35] R. Van Dantzig and L. A. Ch. Koerts, *Nucl. Phys.* **48**, 177 (1963).
- [36] L. N. Generalov, S. N. Abramovich, and A. G. Zvenigorodskij, *J. Izv. Ross. Akad. Nauk, Ser. Fiz.* **64**, 440 (2000).
- [37] G. Perrin, Nguyen Van Sen, J. Arvieux *et al.*, *Nucl. Phys. A* **282**, 221 (1977).
- [38] E. Newman, L. C. Becker, and B. M. Preedom, *Nucl. Phys. A* **100**, 225 (1967).
- [39] F. Hinterberger, G. Mairle, U. Schmidt-Rohr *et al.*, *Nucl. Phys. A* **111**, 265 (1968).
- [40] S. N. Abramovich, B. Ja. Guzhovskij, B. M. Dzuba *et al.*, *J. Izv. Ross. Akad. Nauk, Ser. Fiz.* **40**, 842 (1976).
- [41] S. Ishida, H. Sakai, and H. Okamura, *Phys. Lett. B* **314**, 279 (1993).
- [42] N. Matsuoka, H. Sakai, T. Saito *et al.*, *Nucl. Phys. A* **455**, 413 (1986).
- [43] W. Fitz, R. Jahr, and R. Santo, *Nucl. Phys. A* **101**, 449 (1967).
- [44] O. Aspelund, G. Hrehuss, A. Kiss *et al.*, *Nucl. Phys. A* **253**, 263 (1975).
- [45] H. G. Bingham, A. R. Zander, K. W. Kemper *et al.*, *Nucl. Phys. A* **173**, 265 (1971).
- [46] A. N. Vereshchagin, I. N. Korostova, and I. P. Chernov, *J. Izv. Ross. Akad. Nauk, Ser. Fiz.* **32**, 623 (1968).
- [47] S. E. Darden, G. Murillo, and S. Sen, *Nucl. Phys. A* **266**, 29 (1976).
- [48] G. Duhamel, L. Marcus, H. Langevin-Joliot *et al.*, *Nucl. Phys. A* **174**, 485 (1971).
- [49] A. A. Cowley, G. Heymann, R. L. Keizer *et al.*, *Nucl. Phys.* **86**, 363 (1966).
- [50] R. G. Summers-Gill, *Phys. Rev.* **109**, 1591 (1958).
- [51] A. C. Betker, C. A. Gagliardi, D. R. Semon, R. E. Tribble, H. M. Xu, and A. F. Zaruba, *Phys. Rev. C* **48**, 2085 (1993).
- [52] H. Lüdecke, Tan Wan-Tjin, H. Werner, and J. Zimmerer, *Nucl. Phys. A* **109**, 676 (1968).
- [53] R. J. Slobodian, *Nucl. Phys.* **32**, 684 (1962).
- [54] H. Okamura, S. Ishida, N. Sakamoto *et al.*, *Phys. Rev. C* **58**, 2180 (1998).
- [55] S. Matsuki, S. Yamashita, K. Fukunaga *et al.*, *J. Phys. Soc. Jpn.* **26**, 1344 (1969).
- [56] C. Bäumer, R. Bassini, A. M. van den Berg *et al.*, *Phys. Rev. C* **63**, 037601 (2001).
- [57] N. Burtebayev, S. V. Artemov, and B. A. Duisebayev, *Phys. At. Nucl.* **73**, 746 (2010).
- [58] H. Guratzsch, J. Slotta, and G. Stiller, *Nucl. Phys. A* **140**, 129 (1970).
- [59] A. Korff, P. Haefner, C. Bäumer *et al.*, *Phys. Rev. C* **70**, 067601 (2004).
- [60] R. J. Peterson, H. C. Bhang, J. J. Hamill *et al.*, *Nucl. Phys. A* **425**, 469 (1984).
- [61] G. G. Ohlsen and R. E. Shamu, *Nucl. Phys.* **45**, 523 (1963).
- [62] N. E. Davison, W. K. Dawson, G. Roy *et al.*, *Can. J. Phys.* **48**, 2235 (1970).
- [63] F. Baldeweg, V. Bredel, H. Guratzsch *et al.*, *Nucl. Phys.* **84**, 305 (1966).
- [64] K. W. Corrigan, R. M. Prior, S. E. Darden *et al.*, *Nucl. Phys. A* **188**, 164 (1972).
- [65] K. Hatanaka, K. Imai, S. Kobayashi *et al.*, *Nucl. Phys. A* **340**, 93 (1980).
- [66] L. I. Galanina, N. S. Zelenskaya, V. M. Lebedev *et al.*, *Phys. At. Nucl.* **70**, 273 (2007).
- [67] V. Burjan, Z. Hons, V. Kroha *et al.*, *J. Phys.: Conf. Ser.* **420**, 012142 (2013).
- [68] B. Efron, *Biometrika* **68**, 589 (1981); *SIAM Rev.* **21**, 460 (1979); P. Diaconis and B. Efron, *Sci. Am.* **248**, 116 (1983).
- [69] H. Al Falou, R. Kanungo, C. Andreoiu *et al.*, *Phys. Lett. B* **721**, 224 (2013).
- [70] K. T. Schmitt, K. L. Jones, S. Ahn *et al.*, *Phys. Rev. C* **88**, 064612 (2013).
- [71] Result from the same experiment as in Ref. [27] (unpublished).
- [72] A. M. Mukhamedzhanov, V. Burjan, M. Gulino *et al.*, *Phys. Rev. C* **84**, 024616 (2011).
- [73] F. Flavigny, A. Gillibert, L. Nalpas *et al.*, *Phys. Rev. Lett.* **110**, 122503 (2013).
- [74] B. Guo (private communication).
- [75] A. Auce, R. F. Carlson, A. J. Cox *et al.*, *Phys. Rev. C* **53**, 2919 (1996).